Climate refugia for Asian elephants in Bhutan lie largely outside the protected-area network

Wangdi[1] and Laxmi Sagar[2]*

[1]Department of Forest and Park Services, Ministry of Energy and Natural Resources, Thimphu, Bhutan, 11001

[2]Department of Forest Science, College of Natural Resources, Royal University of Bhutan, Lobesa, Punakha, 14001.

*Corresponding author: sagarlssagar19@gmail.com

Abstract

Bhutan maintains one of the highest proportions of protected-area (PA) coverage globally; however, whether this network effectively safeguards climate-resilient elephant habitat for the Asian elephant (Elephas maximus) remains untested within a nationally consistent modelling framework. We quantified present and future habitat suitability across Bhutan using an ensemble of four algorithms—generalised linear models, random forests, boosted regression trees, and maximum entropy—calibrated with 252 verified presences and 837 verified absences against 17 predictors. Future projections incorporated 96 CMIP6 climate scenarios (8 general circulation models × 4 shared socioeconomic pathways × 3 periods). All models exhibited strong discriminatory performance relative to null expectations (AUC = 0.922–0.960; Boyce Index = 0.964–1.000; all empirical p < 0.010). Precipitation variables dominated model structure, with precipitation of the warmest quarter (BIO18) ranking highest in three algorithms and precipitation of the driest month (BIO14) in the GLM, indicating that seasonal moisture regimes primarily constrain elephant distribution. At the ensemble threshold (0.174), 4,670 km² (14.2% of Bhutan) was classified as suitable habitat, of which 42.9% occurred within PAs and 57.1% outside. Projected habitat change ranged from −6.3% to +19.0% across scenarios. Core climatic refugia covered 4,160 km² (12.6% of Bhutan), with 53.6% located outside the PA network. Mean human–elephant conflict risk increased from 0.103 at present to 0.140 under SSP5–8.5 by 2071–2100, based on 151 georeferenced incidents. These results demonstrate a persistent mismatch between climatically suitable habitat and PA coverage, identifying Bhutan's southern lowland belt as a priority landscape for connectivity planning and conflict mitigation under climate change.

Keywords: climate change; species distribution modelling; climate refugia; human–elephant conflict; protected area effectiveness; habitat suitability

1. Introduction

The Asian elephant (*Elephas maximus* Linnaeus, 1758) is a flagship species of global conservation concern and is currently listed as Endangered on the IUCN Red List of Threatened Species (Choudhury et al., 2008). Global wild populations are estimated at 40,000–50,000 individuals, representing a decline exceeding 50% over three generations driven primarily by habitat loss, fragmentation, and escalating human–wildlife conflict (HWC) (Choudhury et al., 2008; Leimgruber et al., 2003; Sukumar, 2006). In the Eastern Himalayan region, elephant populations occupy highly heterogeneous landscapes spanning steep altitudinal and climatic gradients, where even modest shifts in precipitation seasonality or thermal regimes can

substantially alter habitat connectivity and resource availability (Williams et al., 2020). Climate change therefore represents an emerging threat multiplier that amplifies existing pressures from land-use change and intensifies the spatial overlap between human settlements and elephant movement corridors (Chen et al., 2011; de Silva & Leimgruber, 2019).

Bhutan forms part of a transboundary elephant landscape linking populations in northeastern India (Assam, Arunachal Pradesh, and West Bengal) with those in Bangladesh and represents the northern limit of elephant distribution within the Eastern Himalayan region (Choudhury et al., 2008). As the world's only carbon-negative country, its constitution mandates a minimum 60% national forest cover and enshrines the principle of Gross National Happiness (GNH) as the framework for national development, placing environmental conservation at the centre of policy. Accordingly, Bhutan's PA network covers 19,965 km² (52% of national area), comprising five national parks, four wildlife sanctuaries, one strict nature reserve, and eight biological corridors, among the highest PA coverage rates globally (Nature Conservation Division [NCD], 2020). Despite this exceptional governance context, Bhutan's elephant population (estimated 500–700 individuals; NCD, 2020) faces mounting pressures from agricultural expansion in the southern Himalayan foothills, increasing infrastructure development, and the progressive penetration of climate change into the montane–tropical ecotonal zone. These pressures are compounded by a structural gap in Bhutan's conservation architecture: the PA network is predominantly configured around high-elevation alpine and temperate ecosystems, leaving the subtropical southern belt, which constitutes the primary elephant habitat, chronically underrepresented in formal protection (NCD, 2020).

Species distribution modelling (SDM), also termed ecological niche modelling, provides a rigorous statistical framework for quantifying species–environment relationships and translating them into spatially explicit predictions of habitat suitability (Elith & Leathwick, 2009; Franklin, 2010). When coupled with climate change projections, SDMs enable prospective conservation planning by identifying areas of committed habitat loss, potential range expansion, and climate-stable refugia, defined as areas projected to remain suitable across emission scenarios (Keppel et al., 2012; Morelli et al., 2020). The application of multi-algorithm ensemble approaches, which combine predictions across algorithms to reduce model-specific uncertainty and improve predictive robustness (Araújo & New, 2007; Hao et al., 2020), has become a methodological standard in the field (Zurell et al., 2020). While SDM studies of Asian elephants have been conducted at regional (Mondal et al., 2023) or range-wide scales (Fernando et al., 2012); no study has applied a full CMIP6 multi-model ensemble with verified field absence data and spatial cross-validation at national scale in Bhutan. Furthermore, no study has examined whether Bhutan's globally exceptional PA network is actually positioned to safeguard elephant habitat under climate change.

Therefore, this study presents the first nationally comprehensive, multi-algorithm ensemble SDM for *Elephas maximus* in Bhutan, integrating true presence-absence field data, CMIP6 future climate projections, and spatially blocked cross-validation to address four conservation-oriented objectives: (1) characterise present-day habitat suitability and its key environmental drivers; (2) project habitat change and quantify associated uncertainty across 96 future climate scenarios; (3) delineate climate-stable refugia and assess their coverage within the PA network; and (4) map current and future human–elephant conflict risk hotspots. The analysis provides a nationally applicable evidence base for integrated human–wildlife conflict management planning, and long-

term protected area management frameworks, while also offering a methodological template applicable to other megafauna in similarly complex montane conservation landscapes.

2. Materials and Methods

2.1 Study area

The study encompassed the full national extent of Bhutan (26.7°–28.3°N, 88.8°–92.1°E; 32,973 km²), a Himalayan country in the Eastern Himalayas characterised by a pronounced altitudinal gradient ranging from approximately 100 m in the subtropical southern foothills to over 7,500 m in the northern alpine zone. Climatic conditions transition from humid subtropical in the south, where mean annual precipitation exceeds 5,000 mm in some valleys, through temperate broadleaf and conifer forests, to alpine shrublands and glaciated terrain at higher elevations. Bhutan's protected-area (PA) network comprises five national parks, four wildlife sanctuaries, one strict nature reserve, and eight biological corridors (NCD, 2020). Elephant habitat is confined to the subtropical southern belt, generally below 1,500 m elevation, and is characterised by subtropical broadleaf forests, alluvial plains, and heterogeneous agricultural mosaics (NCD, 2020). All spatial analyses were conducted in EPSG:32645 (WGS 84 / UTM Zone 45N) (Figure 1).

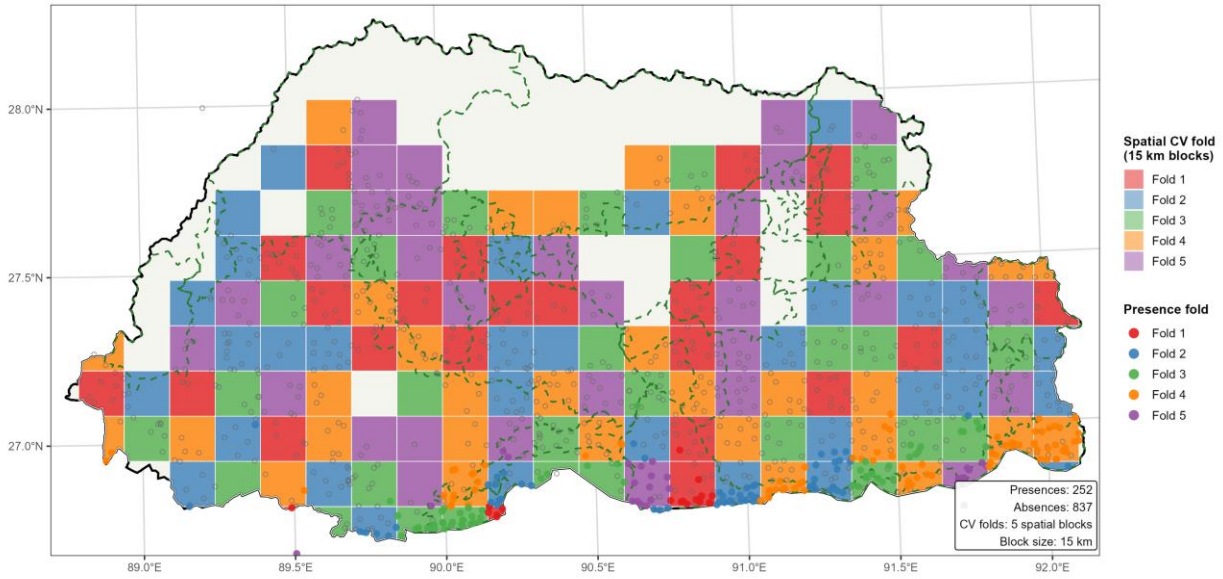

Figure 1. Study area and spatial cross-validation design for Elephas maximus SDM in Bhutan. Bhutan national boundary (black outline); protected area boundaries (dashed green); five-fold spatially blocked cross-validation structure (15 km blocks, coloured by fold assignment: Fold 1 red, 2 blue, 3 green, 4 orange, 5 purple). Filled circles = presence records (n = 252), coloured by fold; open circles = absence records (n = 837). Records are concentrated in the subtropical southern belt. All spatial analysis in EPSG:32645 (WGS 84 / UTM Zone 45N).

2.2 Occurrence data

Occurrence records were derived from national elephant and tiger survey datasets based on a systematic camera-trap network distributed across Bhutan. Camera stations were arranged on an approximately 5 km × 5 km grid, providing near-complete national coverage. A total of 1,089 station-level presence–absence records were compiled from these survey data. Each station was classified as a presence when *Elephas maximus* was detected during at least one sampling event

and as an absence when no detections were recorded. The processing workflow applied coordinate validity checks followed by exact-coordinate deduplication conducted separately for presence and absence records. No pseudo-absence generation was implemented, and no additional spatial thinning was applied beyond duplicate removal, ensuring that each station represented an independent sampling unit. This procedure yielded 252 presence records and 837 verified absences, corresponding to a *presence:absence* ratio of 1:3.32 (Table S14; Figure S10).

2.3 Environmental predictors

A total of 35 candidate predictor variables were compiled across four domains. The climate domain included 19 bioclimatic variables representing baseline conditions for 1986–2015 (hereafter 'present-day' throughout this study), derived from the high-resolution (250 m) CMIP6-based air temperature and precipitation grids for Bhutan developed by Dorji et al. (2025). Topographic variables included elevation (TanDEM-X 12.5 m ALOS DEM), slope, aspect, and terrain ruggedness index (TRI). To account for vegetation and land cover the annual mean Enhanced Vegetation Index (EVI; MOD13Q1, 2000–2024), annual mean Normalised Difference Vegetation Index (NDVI; MOD13Q1, 2000–2024), and a land-cover probability layer (Google Dynamic World 10 m, 2025 composite; Brown et al., 2022) was utilised. Anthropogenic and hydrological factors were represented by the Human Influence Index (HII, 2020 update; WCS/CIESIN, 2005) and Euclidean distances to major rivers, streams, water sources, settlements, protected area boundaries, and private land (cadastral boundaries). Environmental predictor statistics at presence versus absence stations, including Cohen's d effect sizes, are provided in Table S2. Road-network variables were initially evaluated as proxies for anthropogenic accessibility but were excluded from the final predictor set following collinearity screening because they exhibited strong correlation with the Human Influence Index and settlement-distance variables ($|r| \geq 0.85$; VIF ≥ 10) and did not provide additional independent explanatory power, thereby risking inflation of model variance.

Collinearity was assessed using Pearson correlation ($|r| \geq 0.85$) and Variance Inflation Factor (VIF ≥ 10), with predictors iteratively removed retaining those with stronger ecological justification and lower intercorrelations. Elevation was removed due to high correlation with maximum temperature ($r = -0.98$ with BIO05), as was NDVI ($r = 0.86$ with Dynamic World probability) and 13 bioclimatic variables with excessive pairwise correlations. This procedure reduced the candidate set to 17 retained predictors: BIO05 (maximum temperature of warmest month), BIO14 (precipitation of driest month), BIO15 (precipitation seasonality), BIO18 (precipitation of warmest quarter), terrain ruggedness index, slope, aspect, Human Influence Index, EVI, Dynamic World land-cover probability, land-cover class, and Euclidean distances to major rivers, streams, water sources, settlements, protected areas, and private land (Table S1; Figure S6; Appendix S2).

2.4 Species distribution modelling

A four-algorithm ensemble SDM was fitted using GLM, Random Forest, BRT, and MaxEnt. The training code implemented the following settings:

1. **GLM**: binomial family with logit link and forward stepwise AIC selection.
2. **Random Forest**: ranger, 1,000 trees, mtry = $\lfloor\sqrt{17}\rfloor = 4$, and min.node.size = 1.
3. **BRT**: gbm, 1,000 trees, interaction depth = 3, shrinkage = 0.01, and bag.fraction = 0.75.
4. **MaxEnt**: official maxent.jar, betamultiplier = 1.5, cloglog output, and feature classes of hinge, product, linear, and quadratic.

Algorithm-specific hyperparameters, software packages, and verification sources are documented in Table S4.

All models were calibrated with five-fold spatially blocked cross-validation (15 km block size; seed = 123458). Out-of-fold predictions were aggregated for evaluation. The present-day ensemble surface was calculated as an AUC-weighted mean across the four algorithms. Optimal binary thresholds were derived separately for each algorithm by maximising TSS on evaluation outputs; the ensemble threshold used for habitat mapping and sensitivity analysis was rounded to 0.174. MaxEnt out-of-fold predictions extended beyond the standard [0,1] range, so its reported threshold was taken from the full-model prediction workflow. Sensitivity of thresholded habitat area to alternative ensemble suitability thresholds is presented in Table S6 and Supplementary Figure S7.

2.5 Model evaluation

Model performance was assessed from out-of-fold predictions using AUC, TSS, Boyce Index, Brier Score, calibration slope, and Moran's I of residuals. Statistical significance was assessed against 99 label-permuted null models. Confusion-matrix metrics (TP, TN, FP, FN, sensitivity, specificity, PPV, and NPV) were computed using each algorithm's own threshold rather than a single common threshold (Table 1).

2.6 Future climate projections

For each SSP–period combination, the ensemble surface was derived as the unweighted mean of the eight GCM-specific projections. Future climate projections were derived from the Bhutan CMIP6 BIOCLIM Dataset (Dorji et al., 2025), a high-resolution (250 m) canonical infrastructure providing bias-corrected bioclimatic variables for all CMIP6 scenarios. GCM diagnostic reliability scores were computed from the ensemble standard deviation and deviation from the scenario mean, retaining model behavior characterizations for diagnostic interpretation while applying unweighted ensemble means to preserve the full projection uncertainty envelope. GCM performance was assessed diagnostically using this composite metric (Table S8; Figure S13). INM-CM5-0 exhibited the highest reliability (0.840), followed by CNRM-CM6-1 (0.804) and MIROC6 (0.796), whereas MRI-ESM2-0 ranked lowest (0.000).

Individual GCM habitat area trajectories across all SSP–period combinations are shown in Figure S14 and tabulated in Table S10. Habitat gain, loss, persistence, and inter-GCM variability were quantified for each SSP–period ensemble surface. Inter-GCM agreement and spread maps for each scenario are provided in Figures S11 and S12, with summary statistics in Table S9. Novel climate exposure was evaluated using MESS/extrapolation analyses for each GCM–scenario combination. The position of future climates relative to the calibration climate space is illustrated using PCA in Supplementary Figure S8. The mean extrapolation fraction across the 12 SSP–period combinations was 0.001260 (0.13% of pixels), with a maximum of 0.001965 (0.20%) under SSP3–7.0 for 2051–2080. Extrapolation fractions by SSP and period are reported in Table S15; the maximum-risk scenario map is shown in Figure S21. Niche similarity between present and future projections was assessed using Schoener's D and Hellinger's I (Table S17).

2.7 Climate refugia identification

Refugia were classified into two categories: core refugia and high-stability refugia. Core refugia were defined as areas that are suitable under present conditions and remain suitable across all 12 future SSP–period mean projections. High-stability refugia were defined as areas that are

currently suitable and retain suitability in at least 75% of future projections (≥9 of 12 scenarios). Protected-area coverage of these refugia classes was assessed by overlaying them with the national protected-area boundary. Refugia classification definitions and area breakdowns are provided in Table S18.

2.8 Human-elephant conflict risk mapping

Human–elephant conflict risk was not derived from a simple suitability × human influence index formulation but from a composite pressure surface. Instead, a composite human-pressure surface was constructed by integrating a normalised human-footprint layer with a settlement-proximity metric. This surface was combined with normalised ensemble habitat suitability and subsequently rescaled to a 0–1 index. Present-day conflict risk was classified into four categories: low (≤0.040), moderate (0.040–0.069), high (0.069–0.164), and very high (>0.164). Model validation was based on a cleaned conflict dataset comprising 151 records collected between 2015 and 2023. Future conflict risk was estimated by applying the same modelling framework to each SSP–period suitability projection.

2.9 Reproducibility

All analyses were implemented in R 4.4.0. Project code and release metadata are available through the public GitHub repository and Zenodo record documented in the Data Accessibility Statement below. Detailed model diagnostics, predictor summaries, scenario outputs, and validation statistics are provided in the Supplementary Material (Figs. S1–S21; Tables S1–S18).

3. Results

3.1 Model performance

All four algorithms substantially outperformed the null-model distributions (empirical $p < 0.010$) and exceeded the project performance floors (Table 1; Figure S2; Figure S4). MaxEnt achieved the highest AUC among the four algorithms (0.960) and the lowest Brier Score (0.080), whereas RF achieved the highest sensitivity (0.960) and NPV (0.986). Calibration slopes ranged from 0.846 (GLM) to 1.292 (RF), with calibration plots provided in Supplementary Figure S3. Moran's I of OOF residuals ranged from 0.099 to 0.217, indicating limited residual spatial autocorrelation after spatial blocking. Spatial residual autocorrelograms confirming minimal autocorrelation after spatial blocking are shown in Figure S20. Fold-level AUC values ranged from 0.877 to 0.989 across the five spatial blocks, although Fold 1 contained only 19 presences and therefore produced the widest fold-level dispersion (Table S5a; Table S5b; Figure S5).

Table 1. Model performance metrics for each algorithm evaluated on out-of-fold predictions using five-fold spatially blocked cross-validation.

Algorithm	AUC	TSS	Boyce Index	Brier Score	Calib. Slope	Moran's I	Threshold	Sensitivity	Specificity	PPV	NPV
GLM	0.922	0.750	0.988	0.096	0.846	0.217	0.162	0.897	0.824	0.606	0.964
RF	0.948	0.819	0.988	0.081	1.292	0.154	0.217	0.960	0.842	0.647	0.986
BRT	0.943	0.795	1.000	0.086	1.279	0.201	0.179	0.921	0.842	0.637	0.972
MaxEnt	0.960	—	0.964	0.080	0.935	0.099	0.140	0.938	0.837	0.632	0.978

AUC = area under the ROC curve; TSS = true skill statistic; Boyce Index = continuous Boyce index; PPV = positive predictive value; NPV = negative predictive value. MaxEnt TSS was not

available from the OOF predictions, and its threshold was therefore carried over from the full-model output. Algorithm-specific full-model predictions are provided in Supplementary Figure S1.

3.2 Environmental drivers of habitat suitability

Precipitation of the warmest quarter (BIO18) was the highest-ranked predictor in RF, BRT, and MaxEnt, whereas precipitation of the driest month (BIO14) ranked first in the GLM (Table S3; Figure 2). These two precipitation variables define the dominant moisture envelope associated with elephant occurrence in Bhutan. Presence stations were warmer, wetter in the driest month, and much wetter in the warmest quarter than absence stations (Table S2), reinforcing the interpretation that Bhutan's elephant habitat is concentrated within warm, seasonally wet southern lowlands. Maximum temperature of the warmest month (BIO05), terrain ruggedness, and distance to protected areas were also consistently ranked among the stronger predictors. Full marginal response curves for all 17 predictors across the four algorithms are provided in Figure S9.

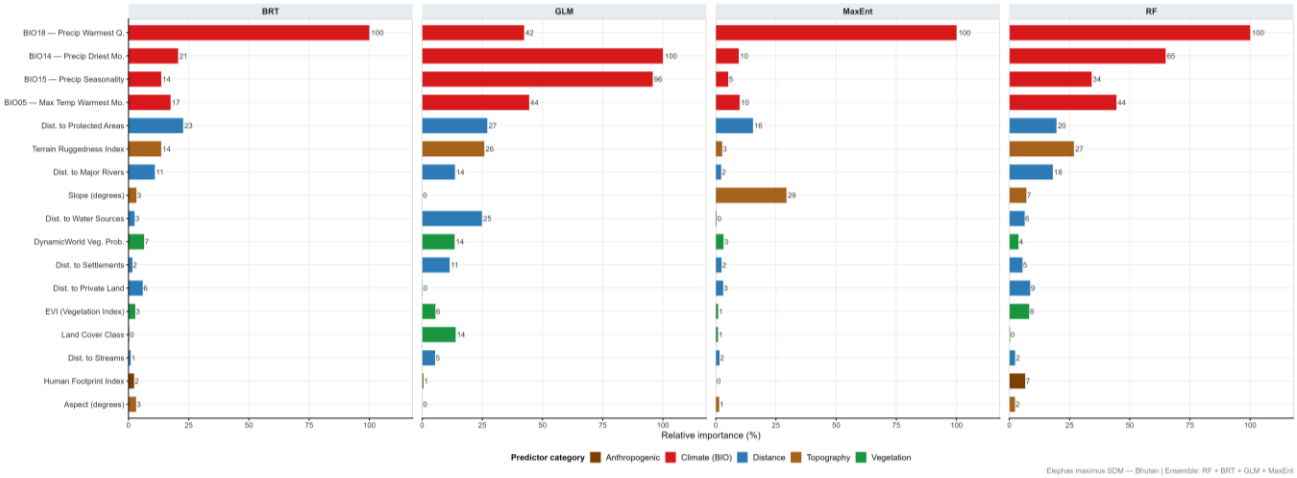

Figure 2. Environmental drivers of Elephas maximus habitat suitability in Bhutan. Normalised variable importance across four algorithms (GLM: coefficient t-statistic; RF: permutation importance; BRT: relative influence; MaxEnt: percent contribution), rescaled so that the maximum within each algorithm equals 100%. BIO18 ranks first in RF, BRT, and MaxEnt, whereas BIO14 ranks first in the GLM.

3.3 Present-day habitat suitability and protected-area coverage

At the ensemble threshold (0.174), the present-day model classified 4,670 km² (14.2% of Bhutan) as suitable habitat (Table 2; Figures 3–4). Suitable areas were concentrated along the southern subtropical belt, extending from Samtse and Chhukha through Dagana, Tsirang, Sarpang, and Zhemgang to Pemagatshel and Samdrup Jongkhar. The largest extents of suitable habitat occurred in Samdrup Jongkhar (1,301.3 km²; 69.4% of district area), Sarpang (966.9 km²; 58.4%), Pemagatshel (602.2 km²; 58.8%), Zhemgang (778.8 km²; 32.5%), and Dagana (446.6 km²; 26.4%) (Table S13). Using the protected-area (PA) union aligned to the 250 m analysis grid, 2,003.8 km² of suitable habitat fell within the PA network and 2,666.5 km² occurred outside, corresponding to 42.9% and 57.1% of the total suitable area, respectively (Table 2). At the individual PA level, Biological Corridor 5, Phibsoo Wildlife Sanctuary, and Jomotsangkha Wildlife Sanctuary were entirely classified as suitable in the overlay analysis, while Royal

Manas National Park contained the largest contiguous block of suitable habitat (837.1 km²; Table S7).

Table 2. Present-day habitat suitability and climate refugia: area, Bhutan-wide coverage, and protected-area status.

Category	Definition	Area (km2)	% of Bhutan	Inside PAs (km2)	% in PAs	Outside PAs (km2)	% outside PAs
Present suitable habitat	Ensemble suitability >= 0.174	4,670	14.2%	2,004	42.9%	2,666	57.1%
Core refugia	Currently suitable and retained in all 12 future scenario means	4,160	12.6%	1,929	46.4%	2,232	53.6%
High-stability refugia	Currently suitable and retained in >=75% of the 12 future scenario means (>=9/12)	4,356	13.2%	1,978	45.4%	2,378	54.6%

The PA percentages in Table 2 are based on the grid-aligned PA union on the 250 m analysis grid (19,793 km²). Per-unit suitable areas in Table S7 are not additive because several corridor and park polygons overlap.

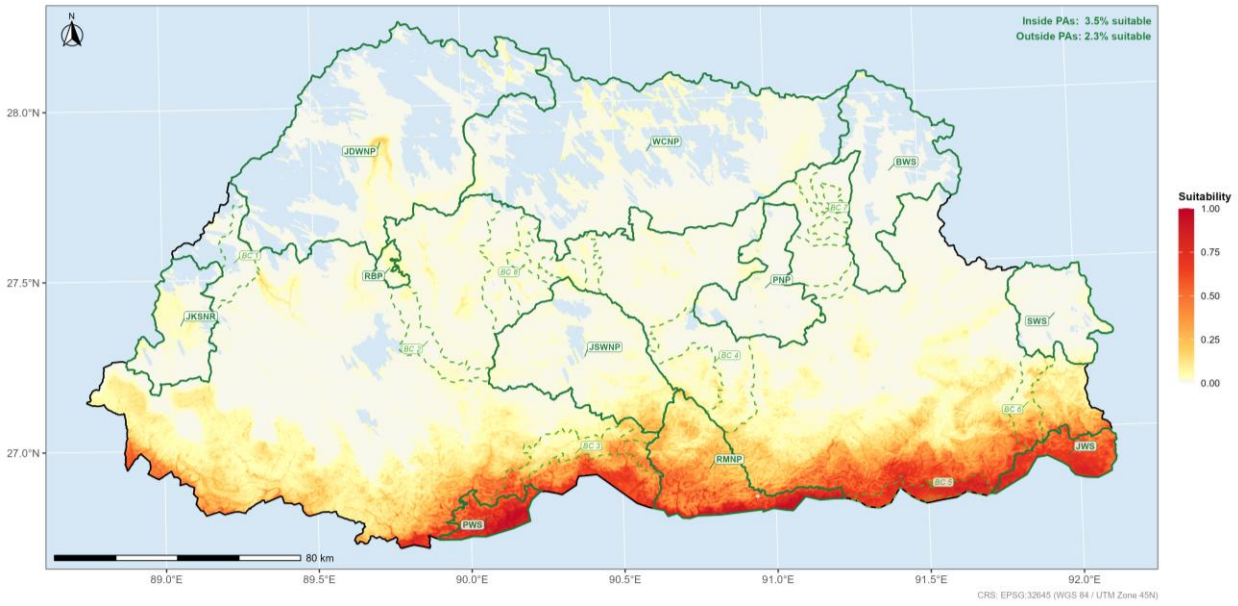

Figure 3. Present-day habitat suitability of Elephas maximus in Bhutan. Ensemble AUC-weighted mean suitability (GLM + RF + BRT + MaxEnt; 1986-2015 climate baseline; EPSG:32645). Using the **grid-aligned PA union** on the 250 m analysis grid, 42.9% of thresholded suitable habitat fell inside the PA network and 57.1% fell outside.

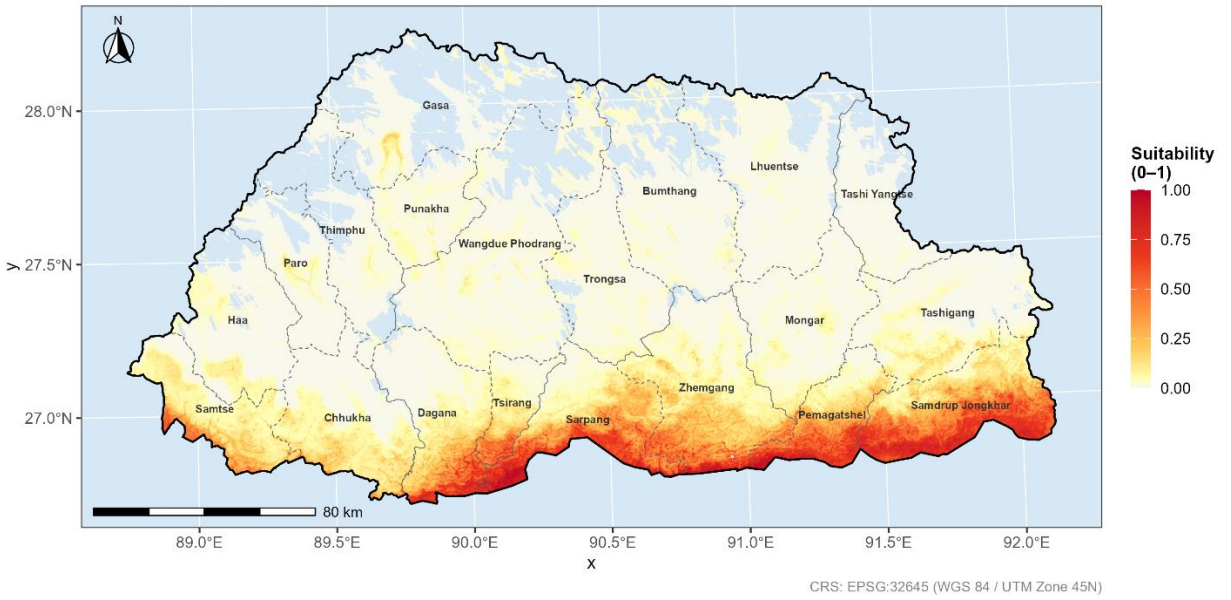

Figure 4. Present-day habitat suitability of *Elephas maximus* in Bhutan. Ensemble model (GLM, RF, BRT, MaxEnt) showing habitat suitability (0–1) under the 1986–2015 baseline. High suitability is concentrated in the southern lowlands. Threshold = 0.174. CRS: EPSG:32645.

3.4 Future habitat trajectories

Future habitat trajectories showed modest scenario-dependent contraction or expansion around the present baseline before stronger expansion in several late-century scenario means (Table 3; Figure 5). Direct recomputation from the SSP–period ensemble surfaces indicated that changes in suitable habitat ranged from −6.3% (SSP5–8.5, 2021–2050) to +19.0% (SSP5–8.5, 2071–2100). Under SSP5–8.5, suitable area declined to 4,377 km² by 2021–2050 before increasing to 5,558 km² by 2071–2100. Under SSP1–2.6, suitable habitat also expanded by late century, reaching 5,543 km². Consequently, low- and high-emissions scenarios converged toward similar total extents of suitable habitat by the end of the century.

Persistence dominated all SSP–period combinations, remaining above 4,224 km² even in the most contraction-prone scenario mean. Gain areas were concentrated along submontane margins, whereas loss areas occurred mainly along the warmest lowland edge. Spatial maps of future ensemble suitability, habitat change, and gain–loss–persistence dynamics for all SSP–period combinations are provided in Figures S15–S17. Inter-GCM uncertainty was highest under SSP5–8.5 by 2071–2100 (mean SD = 0.0421; maximum SD = 0.2132; 11.3% of pixels with SD > 0.10; Table S9), with corresponding spatial uncertainty patterns shown in Figure S18. Niche similarity with the present projection remained high across all scenario means (Schoener's D = 0.7913–0.8670; Hellinger's I = 0.9684–0.9851; Table S17).

Table 3. Projected habitat area, net change, gain, loss, and persistence for *Elephas maximus* in Bhutan under four SSPs and three time periods. Net change is relative to the present-day thresholded area of 4,670 km^2 at threshold 0.174.

SSP	Period	Total area (km^2)	Net change (%)	Gain (km^2)	Loss (km^2)	Persistence (km^2)	GCM SD (mean)

SSP	Period	Total area (km^2)	Net change (%)	Gain (km^2)	Loss (km^2)	Persistence (km^2)	GCM SD (mean)
SSP1-2.6	2021-2050	4,621	-1.1%	259	309	4,361	0.021
SSP1-2.6	2051-2080	5,149	+10.2%	564	85	4,585	0.024
SSP1-2.6	2071-2100	5,543	+18.7%	912	39	4,632	0.031
SSP2-4.5	2021-2050	4,694	+0.5%	302	279	4,392	0.021
SSP2-4.5	2051-2080	4,894	+4.8%	450	226	4,444	0.022
SSP2-4.5	2071-2100	5,430	+16.3%	833	73	4,597	0.037
SSP3-7.0	2021-2050	4,882	+4.5%	546	334	4,336	0.017
SSP3-7.0	2051-2080	4,811	+3.0%	432	291	4,379	0.027
SSP3-7.0	2071-2100	4,704	+0.7%	383	349	4,321	0.028
SSP5-8.5	2021-2050	4,377	-6.3%	152	446	4,225	0.016
SSP5-8.5	2051-2080	5,028	+7.7%	532	175	4,496	0.033
SSP5-8.5	2071-2100	5,558	+19.0%	957	69	4,601	0.042

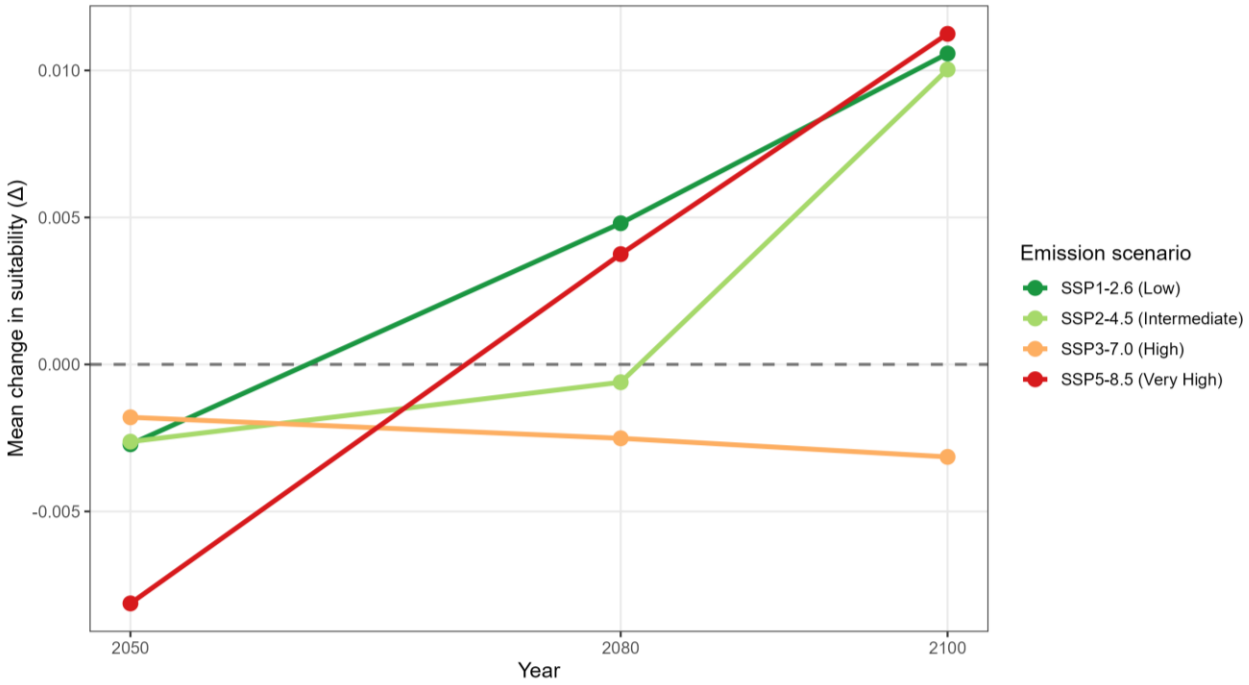

Figure 5. Future habitat trajectories for Elephas maximus in Bhutan across four Shared Socioeconomic Pathways (2021-2100). Lines show the simple across-GCM mean habitat area for each SSP-period combination; shading indicates plus/minus 1 SD across GCMs. The horizontal dashed line denotes the present-day baseline of 4,670 km^2 (14.2% of Bhutan).

3.5 Climate refugia

The refugia products identified 4,160 km^2 (12.6% of Bhutan) as core refugia, interpreted here as currently suitable pixels retained across all 12 future SSP-period mean surfaces (Table 2; Table S18; Figure 6). The high-stability class covered 4,356 km^2 (13.2% of Bhutan) and is best interpreted as currently suitable pixels retained in at least 75% of the 12 future scenario means.

Core refugia were concentrated in the same southern lowland arc as the present suitability surface. The overlay indicated that 46.4% of core refugia and 45.4% of high-stability refugia fell inside the PA network, leaving slightly more than half of each class outside formal protection. Refugia stability-class area breakdowns are detailed in Table S18.

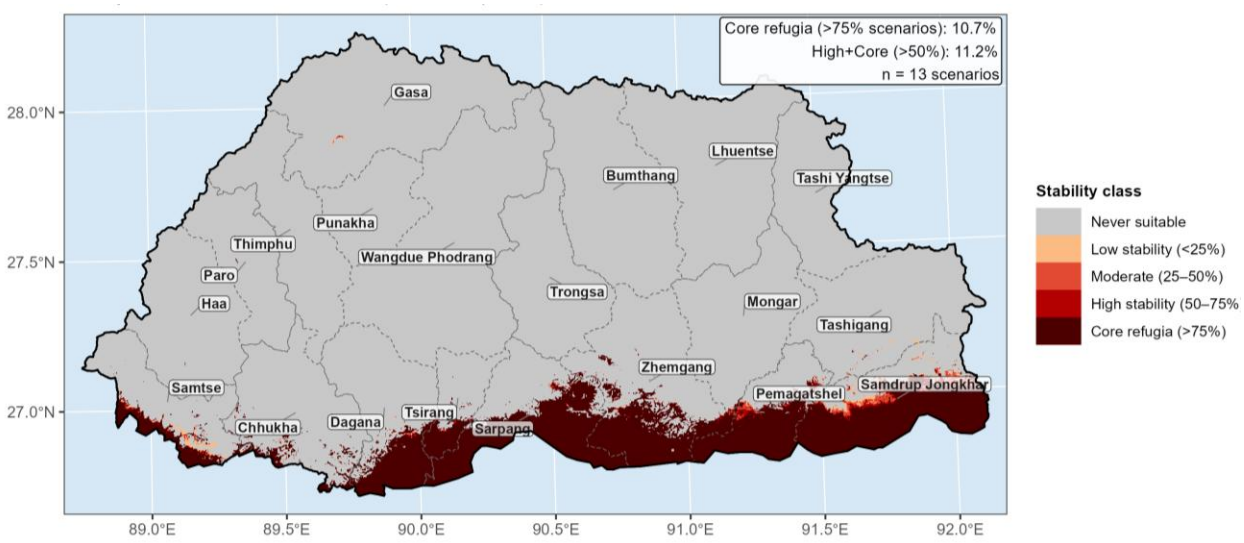

Figure 6. Climate refugia stability classification for Elephas maximus in Bhutan. The mapped core-refugia product identifies pixels that remained suitable across the scenario set. For reporting, core refugia are interpreted as currently suitable pixels retained in all 12 future scenario means. Core refugia covered 4,160 km^2, of which 46.4% fell inside the PA network.

3.6 Human-elephant conflict risk - present and future

Present-day risk mapping classified 11,541 km^2 (35% of Bhutan) as high or very high conflict risk (high: 6,595 km^2; very high: 4,946 km^2; Table S11; Figure 7). The cleaned conflict archive contained 151 records, of which 73 were crop-damage incidents, 32 were property-damage incidents, and 46 were coded as other damage types. The incident file contained no usable casualty_type coding. Recorded incidents were most frequent in Samdrup Jongkhar (50 records) and Sarpang (46), with smaller counts in Zhemgang, Chukha, Dagana, Tsirang, Pemagatshel, and Samtse; 26 records lacked district coding.

Future mean conflict risk increased across all four SSPs and all three future periods (Table S11 & S12; Figure S19). The mean risk index rose from 0.103 at present to 0.127 under SSP1-2.6 by 2071-2100 and to 0.140 under SSP5-8.5 by 2071-2100, a 35.9% increase relative to the present baseline. The end-century mean under SSP2-4.5 (0.132) slightly exceeded that under SSP3-7.0 (0.129), indicating that the risk surface was not ordered strictly by radiative forcing. Spatial coincidence between refugia and elevated conflict risk remained a central management issue in the verified outputs.

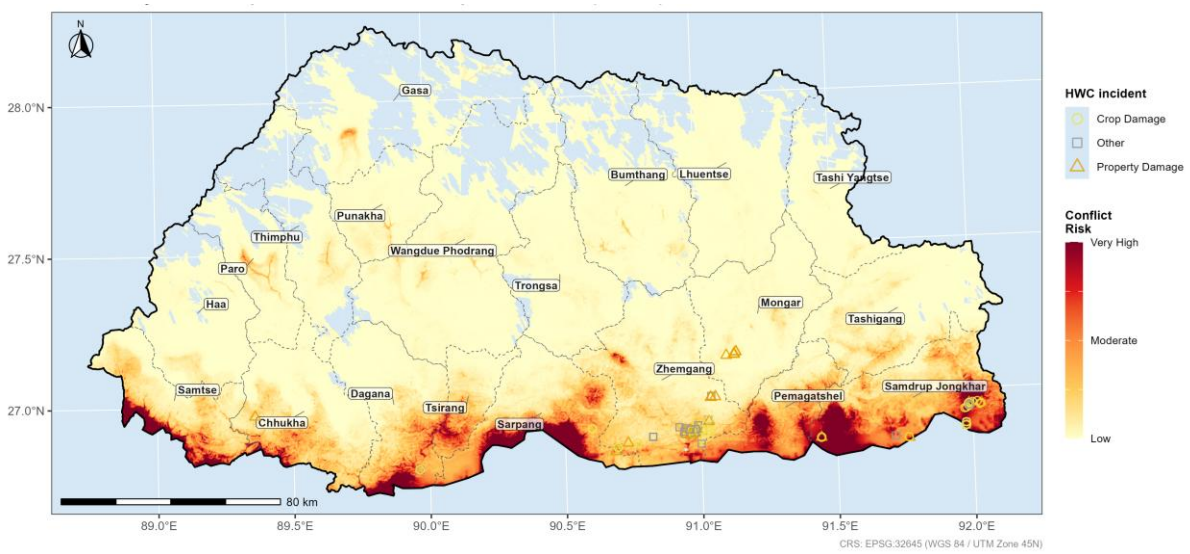

Figure 7. Present-day human-elephant conflict risk in Bhutan. Risk was derived from normalised ensemble suitability multiplied by a human-pressure surface that combined human footprint and settlement proximity, then re-normalised to [0,1]. The cleaned conflict archive contained 151 incident records. High or very high-risk zones covered 11,541 km^2 (35% of Bhutan).

4. Discussion

4.1 The subtropical moisture envelope as the primary habitat determinant

The results demonstrate that the precipitation regime—specifically the amplitude of the monsoon peak (BIO18) and the severity of the dry-season minimum (BIO14)—is the primary determinant of Asian elephant habitat suitability in Bhutan, with BIO18 ranked first in three of four algorithms. This pattern is ecologically coherent: monsoon-season rainfall (BIO18) drives peak forage productivity, supporting fat accumulation and body condition necessary for reproduction and calf survival (Sukumar, 1989; Campos-Arceiz & Blake, 2011). Dry-season precipitation (BIO14) governs the persistence of water sources and patchily distributed riparian vegetation during the November–April lean season, thereby constraining the southern boundary of the viable year-round range (de Silva & Leimgruber, 2019). Together, BIO18 and BIO14 define a subtropical moisture envelope within which elephant habitat in Bhutan is embedded. BIO05 (maximum temperature of the warmest month) characterises the thermal conditions of this envelope, whereas BIO18 and BIO14 define its moisture constraints. Suitable habitat thus occurs where conditions are sufficiently warm to sustain monsoon-driven productivity and sufficiently moist to maintain dry-season resource availability.

However, these findings contrast with Mondal et al. (2023), who identified temperature variables as dominant in sub-Himalayan Bengal (India), reflecting the lower elevational range and more temperature-limited conditions of the Ganges foothills. In Bhutan's montane system, where temperature varies continuously with elevation, accessible elephant habitat is effectively restricted to a narrow thermal band. Within this band, precipitation variability—rather than temperature per se—emerges as the principal determinant of habitat quality. The relatively low importance of human footprint at the national scale (0.1–6.6% across algorithms), despite well-documented sensitivity of elephants to anthropogenic pressure (Barua et al., 2013), likely reflects the comparatively intact landscape of southern Bhutan rather than a lack of biological response.

The detection of unusually high slope importance in MaxEnt (29.4% versus <8% in other algorithms) warrants a methodological note. MaxEnt's feature-type interactions (linear, quadratic, hinge, and product) can generate complex implicit variable combinations. In low-slope lowland terrain—where elephant occurrence is concentrated—slope co-varies with accessibility and agricultural development in ways not captured by single-variable importance metrics in other algorithms. This pattern is therefore interpreted as a modelling artefact rather than an independent ecological signal.

4.2 The protected-area coverage paradox

The verified present-day ensemble surface classified 4,670 km² of Bhutan as suitable elephant habitat, concentrated in the southern foothills. Using the grid-aligned PA union, 57.1% of that suitable habitat occurred outside the PA network. This distribution indicates that a large share of Bhutan's elephant habitat lies in multiple-use southern landscapes rather than within the core protected-area system. Such a pattern reflects a structural feature of PA configuration rather than an incidental omission. Bhutan's protected areas were predominantly established to conserve high-elevation temperate, alpine, and nival ecosystems, consistent with the well-documented global bias toward locating protected areas in remote, low-opportunity-cost terrain (Joppa & Pfaff, 2009; Venter et al., 2018). While this strategy maximises forest cover and carbon retention, it systematically underrepresents lowland megafauna whose ranges overlap with productive agricultural landscapes (Fernando et al., 2012).

Biological Corridor 5 and Jomotsangkha Wildlife Sanctuary together account for approximately 591 km² of suitable habitat in the per-unit overlay summary; however, because protected-area polygons overlap, these values are not strictly additive. Even so, this combined extent represents only about 12.7% of total suitable habitat and is therefore unlikely, on its own, to secure the southern habitat belt. Comparable patterns are reported across the Asian elephant range, including India (Choudhury et al., 2008; Mondal et al., 2023) and Sri Lanka (Fernando et al., 2012), where the majority of suitable habitat occurs outside strictly protected areas in human-dominated landscapes. The policy implication is not that Bhutan's PA system is ineffective, but that a high-coverage PA estate—largely configured around montane ecosystems—does not fully align with the spatial requirements of a lowland megaherbivore. This mismatch remains both ecological and political because the same southern landscapes also support agriculture, settlements, and transport infrastructure. Under the Kunming–Montreal Global Biodiversity Framework (Target 3, "30×30"), this gap presents an opportunity to expand conservation through Other Effective Area-Based Conservation Measures (OECMs) across community forests, private lands, and agricultural mosaics.

For Bhutan specifically, however, this gap represents not merely a spatial mismatch but a governance challenge. Southern dzongkhags—including Samdrup Jongkhar, Pemagatshel, and Sarpang—where elephant habitat is most concentrated, are also areas of high agricultural activity and increasing human pressure, intensifying human–elephant conflict (Tshering et al., 2024). In the private-land overlay, cadastral polygons cover 2,261.5 km² and exhibit a mean suitability of 0.102, indicating that coexistence-oriented management outside strict PAs remains necessary. These landscapes therefore represent not only a conservation opportunity but a socio-political interface where OECMs must reconcile livelihood needs with species conservation objectives.

4.3 Climate resilience, refugia, and late-century convergence

The modelled elephant niche remains relatively stable across future climate means, as indicated by high Schoener's D and Hellinger's I value and low MESS/extrapolation fractions. Late-century total habitat area converges to similar magnitudes under SSP1–2.6 and SSP5–8.5 despite strongly divergent emission pathways. Under SSP5–8.5, suitable habitat contracts most strongly by 2021–2050 before expanding to 5,558 km² by 2071–2100, whereas under SSP1–2.6 it reaches 5,543 km² by the end of the century (Table 3). The key conservation distinction therefore lies in the trajectory rather than the endpoint: the near-term contraction under high emissions represents a potential population bottleneck for a slow-reproducing megaherbivore. This dynamic is consistent with evidence that climate-driven range shifts in montane systems are often governed by upslope expansion of thermal envelopes (Chen et al., 2011; Telwala et al., 2013), while long-term responses are partly constrained by committed warming under existing emission trajectories (Matthews & Caldeira, 2008).

Core refugia provide the most defensible spatial basis for long-term conservation planning. The core-refugia surface covers 4,160 km², with 46.4% located within the PA network and 53.6% outside formal protection (Table 2). Because these areas remain suitable across all SSP–period means, they represent priority zones for corridor protection, coexistence-oriented management, and climate-resilient land-use planning. The fact that more than half of these refugia lie outside formal protection highlights a persistent conservation gap and reinforces the need to extend management beyond the existing PA network.

4.4 The climate-conflict nexus

The conflict outputs indicate a clear climate–conflict nexus, although earlier interpretations overstated the strength of evidence. The cleaned conflict archive contains 151 records (not 152), with coded damage types limited to crop damage, property damage, and other categories. These incidents are concentrated in the same southern districts that dominate present-day suitability, particularly Samdrup Jongkhar and Sarpang. The modelled risk surface increases across all SSP–period means, rising from 0.103 at present to 0.140 under SSP5–8.5 by 2071–2100, representing a 35.9% increase in the spatial coincidence of habitat suitability and human exposure (Table S12) . The slight inversion between SSP2–4.5 and SSP3–7.0 in late-century risk levels indicates that conflict escalation is not strictly proportional to radiative forcing, but likely reflects interactions between precipitation dynamics and local habitat shifts. The spatial overlap between climatically persistent habitat and elevated conflict risk defines a central conservation constraint. Areas most likely to support long-term elephant persistence are also those where human–elephant interactions are already concentrated. This does not reduce the importance of refugia; rather, it requires that refugia protection and conflict mitigation be implemented as coupled strategies. Evidence from South Asian contexts indicates that measures such as solar-powered electric fencing, early warning systems linked to elephant movement, rapid response mechanisms, and compensation or insurance schemes are effective in maintaining coexistence where exposure is high (Wangchuk, 2004; Wang & Macdonald, 2006; Barua et al., 2013).

Within Bhutan's governance framework, this overlap presents a structural challenge. Southern dzongkhags—including Samdrup Jongkhar, Pemagatshel, and Sarpang—anchor both core refugia and the highest conflict risk, while also supporting intensive agriculture and rural livelihoods. In these settings, crop loss from elephants can represent a substantial share of household income, elevating the socio-economic stakes of conservation interventions. Conflict mitigation infrastructure in these landscapes is therefore not a secondary component of

conservation planning but a prerequisite for sustaining long-term coexistence and ensuring that climate-resilient habitats remain socially viable.

4.5 Methodological considerations

Several strengths of the workflow remain intact after validation: true field absences were used rather than pseudo-absences, spatial block cross-validation constrained spatial leakage, multiple evaluation metrics were reported, and the full 8 GCM × 4 SSP × 3 period design was successfully completed. Compliance with the ODMAP protocol for species distribution model reporting (Zurell et al., 2020) is summarised in Table S16, with the full protocol provided in Supplementary Appendix S1. The code audit also clarified several methodological details that required correction in the manuscript. No additional 5 km thinning was applied to occurrences; BRT used bag.fraction = 0.75; confusion-matrix metrics were derived from algorithm-specific thresholds; and future SSP–period ensemble surfaces were computed as simple unweighted means across GCMs rather than reliability-weighted means.

The audit also exposed several caveats. The present suitability and district summaries differ slightly because thresholding and polygon aggregation are not identical operations. The PA network percentages used for conservation inference are therefore tied explicitly to the grid-aligned PA union on the 250 m analysis grid. Similarly, the conflict-risk formulation incorporated settlement proximity in addition to the human-footprint layer, and the clean conflict file did not preserve usable casualty-type coding. These do not invalidate the main conclusions, but they do constrain how precisely some manuscript statements can be framed.

5. Conclusions

This audit confirms the core ecological message of the study while tightening the quantitative interpretation. The verified present-day ensemble surface classified 4,670 km² of Bhutan as suitable elephant habitat, concentrated in the southern foothills. Using the grid-aligned PA union, 57.1% of that suitable habitat occurred outside the PA network. Future scenario means showed relatively limited climatic novelty, strong overlap with the present niche, and late-century expansion under several SSPs, but they also highlighted near-term contraction under SSP5–8.5 and persistent conservation dependence on the southern lowland belt.

Core refugia covered 4,160 km², with 53.6% located outside the PA network. At the same time, the conflict-risk surface increased from 0.103 at present to 0.140 under SSP5–8.5 by 2071–2100, and the cleaned conflict archive showed that southern districts already contained most documented incidents. The resulting policy message is clear: Bhutan’s elephant conservation strategy should prioritise southern landscape connectivity, protection or co-management of unprotected refugia, and conflict mitigation in the same landscapes where long-term climatic persistence is most likely.

Acknowledgements

The authors thank the Department of Forest and Park Services (NCD) for providing occurrence data, protected-area boundaries, and conflict records. The BhutanBioClims dataset was used to derive the climate predictors, and Dynamic World and MODIS products supported the land-cover and vegetation components of the workflow.

Author Contributions

Wangdi: Conceptualisation, Methodology, Software, Formal analysis, Visualisation, Investigation, Data Curation, Writing - Original Draft. **Laxmi Sagar**: Resources, Investigation, Validation, Writing - Review and Editing.

Competing Interests

The authors declare no competing interests.

Funding

This research received no external funding. The study was conducted as part of institutional research activities supported by the Department of Forest and Park Services, Royal Government of Bhutan.

Data Accessibility Statement

Code, configuration, and tabular outputs are available from the public GitHub repository (https://github.com/wangdiues/Elephas_maximus_SDM_Project_v4) and the Zenodo software archive for version v0.1.0 (https://doi.org/10.5281/zenodo.19659305; concept DOI https://doi.org/10.5281/zenodo.19659304). Climate model inputs were derived from the high-resolution Bhutan dataset of Dorji et al. (2025), which provides 250 m historical and CMIP6-projected air temperature and precipitation grids (DOI: 10.25919/pec2-hs50). Sensitive wildlife occurrence coordinates and conflict-point data are not redistributed publicly because they contain species-location and incident-location information; access requests should be directed to the Department of Forest and Park Services, subject to data-governance approvals.

References

Araújo, M. B., & New, M. (2007). Ensemble forecasting of species distributions. *Trends in Ecology & Evolution*, *22*(1), 42–47. https://doi.org/10.1016/j.tree.2006.09.010

Barua, M., Bhagwat, S. A., & Jadhav, S. (2013). The hidden dimensions of human–wildlife conflict: health impacts, opportunity and transaction costs. *Biological Conservation*, *157*, 309–316. https://doi.org/10.1016/j.biocon.2012.07.014

Breiman, L. (2001). Random forests. *Machine Learning*, *45*(1), 5–32. https://doi.org/10.1023/A:1010933404324

Brown, C. F., Brumby, S. P., Guzder-Williams, B., Birch, T., Hyde, S. B., Mazzariello, J., Tait, A. M., ... & Williams, M. (2022). Dynamic World, near real-time global 10 m land use land cover mapping. *Scientific Data*, *9*(1), Article 251. https://doi.org/10.1038/s41597-022-01307-4

Campos-Arceiz, A., & Blake, S. (2011). Megagardeners of the forest: The role of elephants in seed dispersal. *Acta Oecologica*, *37*(6), 542–553. https://doi.org/10.1016/j.actao.2011.01.014

Chen, I.-C., Hill, J. K., Ohlemüller, R., Roy, D. B., & Thomas, C. D. (2011). Rapid range shifts of species associated with high levels of climate warming. *Science*, *333*(6045), 1024–1026. https://doi.org/10.1126/science.1206432

Choudhury, A., Lahiri Choudhury, D. K., Desai, A., Duckworth, J. W., Easa, P. S., Johnsingh, A. J. T., ... & Wijesundara, S. (2008). *Elephas maximus* (errata version published in 2011). The IUCN Red List of Threatened Species 2008: e.T7140A12828813. https://www.iucnredlist.org/species/7140/12828813

de Silva, S., & Leimgruber, P. (2019). Demographic tipping points as early indicators of vulnerability for slow-breeding megafaunal populations. *Frontiers in Ecology and Evolution*, *7*, Article 171. https://doi.org/10.3389/fevo.2019.00171

Nature Conservation Division, Department of Forests and Park Services, Ministry of Agriculture and Forests. (2018). National elephant survey report. Nature Conservation Division, Department of Forests and Park Services, Ministry of Agriculture and Forests.

Dorji, Sangay; Stewart, Stephen; Bajwa, Ali; Aziz, Ammar; Shabbir, Asad; & Adkins, Steve (2025): High-resolution (250 m) historical and projected (CMIP6) air temperature and precipitation grids for Bhutan. v1. CSIRO. Data Collection. https://doi.org/10.25919/pec2-hs50

Elith, J., Graham, C. H., Anderson, R. P., Dudík, M., Ferrier, S., Guisan, A., ... & Zimmermann, N. E. (2006). Novel methods improve prediction of species' distributions from occurrence data. *Ecography*, *29*(2), 129–151. https://doi.org/10.1111/j.2006.0906-7590.04596.x

Elith, J., Leathwick, J. R., & Hastie, T. (2008). A working guide to boosted regression trees. *Journal of Animal Ecology*, *77*(4), 802–813. https://doi.org/10.1111/j.1365-2656.2008.01390.x

Elith, J., & Leathwick, J. R. (2009). Species distribution models: Ecological explanation and prediction across space and time. *Annual Review of Ecology, Evolution, and Systematics*, *40*, 677–697. https://doi.org/10.1146/annurev.ecolsys.110308.120159

Elith, J., Kearney, M., & Phillips, S. (2010). The art of modelling range-shifting species. *Methods in Ecology and Evolution*, *1*(4), 330–342. https://doi.org/10.1111/j.2041-210X.2010.00036.x

Fernando, P., Wikramanayake, E., Weerakoon, D., Jayasinghe, L. K. A., Gunawardene, M., & Janaka, H. K. (2005). Perceptions and patterns of human–elephant conflict in old and new settlements in Sri Lanka. *Biodiversity and Conservation*, *14*(10), 2465–2481. https://doi.org/10.1007/s10531-004-0216-z

Franklin, J. (2010). *Mapping species distributions: Spatial inference and prediction*. Cambridge University Press.

Friedman, J. H. (2001). Greedy function approximation: a gradient boosting machine. *Annals of Statistics*, *29*(5), 1189–1232. https://doi.org/10.1214/aos/1013203451

Guisan, A., Edwards, T. C., & Hastie, T. (2002). Generalised linear and additive models in studies of species distributions. *Ecological Modelling*, *157*(2–3), 89–100. https://doi.org/10.1016/S0304-3800(02)00204-1

Hao, T., Elith, J., Guillera-Arroita, G., & Lahoz-Monfort, J. J. (2020). Testing whether ensemble modelling improves predictive performance. *Ecography*, *43*(4), 549–558. https://doi.org/10.1111/ecog.04890

Hirzel, A. H., & Le Lay, G. (2008). Habitat suitability modelling and niche theory. *Journal of Applied Ecology*, *45*(5), 1372–1381. https://doi.org/10.1111/j.1365-2664.2008.01524.x

Hirzel, A. H., Le Lay, G., Helfer, V., Randin, C., & Guisan, A. (2006). Evaluating habitat suitability models. *Ecological Modelling*, *199*(2), 142–152. https://doi.org/10.1016/j.ecolmodel.2006.05.017

Joppa, L. N., & Pfaff, A. (2009). High and far: biases in protected areas. *PLoS ONE*, *4*(12), Article e8273. https://doi.org/10.1371/journal.pone.0008273

Keppel, G., Van Niel, K. P., Wardell-Johnson, G. W., Yates, C. J., Byrne, M., Mucina, L., ... & Franklin, S. E. (2012). Refugia under climate change. *Global Ecology and Biogeography*, *21*(4), 393–404. https://doi.org/10.1111/j.1466-8238.2011.00686.x

Leimgruber, P., Gagnon, J. B., Wemmer, C., Kelly, D. S., Songer, M. A., & Selig, E. R. (2003). Fragmentation of Asia's remaining wildlands: implications for Asian elephant conservation. *Animal Conservation*, *6*(4), 347–359. https://doi.org/10.1017/S1367943003003421

Matthews, H. D., & Caldeira, K. (2008). Stabilizing climate requires near-zero emissions. *Geophysical Research Letters*, *35*(4), Article L04705. https://doi.org/10.1029/2007GL032388

Merow, C., Smith, M. J., & Silander, J. A. (2013). Practical guide to MaxEnt. *Ecography*, *36*(10), 1058–1069. https://doi.org/10.1111/j.1600-0587.2013.07872.x

Mondal, I., Thakur, S., Ghosh, P., & Bandyopadhyay, J. (2023). Modelling Asian elephant distribution. *Ecological Informatics*, *73*, Article 101930. https://doi.org/10.1016/j.ecoinf.2022.101930

Morelli, T. L., Barrows, C. W., Ramirez, A. R., Cartwright, J. M., Ackerly, D. D., Eaves, T. D., Ebersole, J. L., Krawchuk, M. A., Letcher, B. H., Mahalovich, M. F., Meigs, G. W., Michalak, J. L., Millar, C. I., Quiñones, R. M., Stralberg, D., & Thorne, J. H. (2020). Climate-change refugia: Biodiversity in the slow lane. *Frontiers in Ecology and the Environment*, *18*(5), 228–234. https://doi.org/10.1002/fee.2189

Phillips, S. J., Anderson, R. P., & Schapire, R. E. (2006). Maximum entropy modelling of species geographic distributions. *Ecological Modelling*, *190*(3–4), 231–259. https://doi.org/10.1016/j.ecolmodel.2005.03.026

Phillips, S. J., Anderson, R. P., Dudík, M., Schapire, R. E., & Blair, M. E. (2017). Opening the black box: an open-source release of Maxent. *Ecography*, *40*(7), 887–893. https://doi.org/10.1111/ecog.03049

R Core Team. (2024). *R: A language and environment for statistical computing*. R Foundation for Statistical Computing. https://www.R-project.org/

Roberts, D. R., Bahn, V., Ciuti, S., Boyce, M. S., Elith, J., Guillera-Arroita, G., ... & Dormann, C. F. (2017). Cross-validation strategies for data with temporal, spatial, hierarchical, or phylogenetic structure. *Ecography*, *40*(8), 913–929. https://doi.org/10.1111/ecog.02881

Sanderson, B. M., Knutti, R., & Caldwell, P. (2015). Addressing interdependency in a multimodel ensemble by interpolation of model properties. Journal of Climate, 28(13), 5150–5170. https://doi.org/10.1175/JCLI-D-14-00361.1

Sukumar, R. (1989). *The Asian elephant: Ecology and management*. Cambridge University Press.

Sukumar, R. (2006). A brief review of the status, distribution and biology of wild Asian elephants *Elephas maximus*. *International Zoo Yearbook, 40*(1), 1–8. https://doi.org/10.1111/j.1748-1090.2006.00001.x

Telwala, Y., Brook, B. W., Manish, K., & Pandit, M. K. (2013). Climate-Induced Elevational Range Shifts and Increase in Plant Species Richness in a Himalayan Biodiversity Epicentre. *PLoS ONE, 8*(2), Article e57103. https://doi.org/10.1371/journal.pone.0057103

Tshering, U., Thakur, R., Ghosh, S., & Nath, A. (2024). Addressing human–elephant conflict in Bhutan: a case study from Sarpang. *Journal of Wildlife Science*. Advance online publication. https://doi.org/10.63033/JWLS.FTLB3638

Valavi, R., Elith, J., Lahoz-Monfort, J. J., & Guillera-Arroita, G. (2019). blockCV: an R package for generating spatially or environmentally separated folds for k-fold cross-validation of species distribution models. *Methods in Ecology and Evolution, 10*(2), 225–232. https://doi.org/10.1111/2041-210X.13107

Venter, O., Magrach, A., Outram, N., Klein, C.J., Possingham, H.P., Di Marco, M. and Watson, J.E.M. (2018), Bias in protected-area location and its effects on long-term aspirations of biodiversity conventions. Conservation Biology, 32: 127-134. https://doi.org/10.1111/cobi.12970

Wang, S. W., & Macdonald, D. W. (2006). Livestock predation by carnivores in Jigme Singye Wangchuck National Park, Bhutan. *Biological Conservation, 129*(4), 558–565. https://doi.org/10.1016/j.biocon.2005.11.024

Wangchuk, T. (2004). Predator-prey dynamics: The role of predators in the control of problem species. *Journal of Bhutan Studies, 10*, 1–15.

Wildlife Conservation Society-WCS, & Center for International Earth Science Information Network-CIESIN-Columbia University. (2005). *Last of the Wild Project, Version 2, 2005 (LWP-2): Global Human Footprint Dataset (IGHP)* (Version 2.00) [Data set]. Palisades, NY: NASA Socioeconomic Data and Applications Center (SEDAC). https://doi.org/10.7927/H4GF0RFQ Date Accessed: 2026-04-22.

Williams, A. C., Johnsingh, A. J. T., & Krausman, P. R. (2001). Elephant–human conflicts in Rajaji National Park, northwestern India. *Wildlife Society Bulletin, 29*(4), 1097–1104.

Zurell, D., Franklin, J., König, C., Bouchet, P. J., Dormann, C. F., Elith, J., ... & Zimmermann, N. E. (2020). A standard protocol for reporting species distribution models. *Ecography, 43*(9), 1261–1277. https://doi.org/10.1111/ecog.04960